JOURNAL OF MATERIALS SCIENCE 23 (1988) 1201–1205

Studies on β-FeOOH

Part 2 *Physico-chemical characteristics of thermally treated akaganeite (β-FeOOH)*

K. M. PARIDA
Regional Research Laboratory, Bhubaneswar 751 013, Orissa, India

Akaganeite is transformed into haematite at 300° C through a quasiamorphous intermediate phase at 200° C. The XRD patterns, crystallite sizes, infrared spectra, conductivity measurements, scanning electron micrographs and density values confirm the presence of an intermediate phase at 200° C. The chloride content decreases sharply between 200 and 300° C and remains with haematite up to 600° C. The quasiamorphous phase possesses the highest surface area, lowest crystallite size, lowest density and diffuse XRD patterns of all the heat-treated products of β-FeOOH.

1. Introduction

Akaganeite (β-FeOOH) is transformed into haematite (α-Fe_2O_3) through dehydration process accompanied by a structural change from tetragonal to rhombohedral. This transformation has been extensively studied by various methods such as X-ray diffraction patterns, infrared spectroscopy, Mössbauer spectroscopy, magnetic analysis, electron microscopy, etc. [1–3]. Dezsi *et al.* [4] and Ishikawa and Inouye [5] reported that β-FeOOH was directly transformed into α-Fe_2O_3 by thermal decomposition. On the other hand, it has been reported that the crystal structure of akaganeite gradually degenerates into a quasiamorphous intermediate state before final phase transformation to Fe_2O_3 takes place [6–8]. According to Nagai *et al.* [3], the intermediate, whose structure is similar to β-FeOOH was antiferromagnetic at temperatures below 470 K. However, no data are available on the physico-chemical parameters of the quasiamorphous intermediate as well as the thermally decomposed products. In the present investigation the isothermal treatment of synthetic akaganeite in air up to 1000° C was carried out and the intermediate products were characterized by means of X-ray powder diffraction (XRD) patterns, infrared spectroscopy, surface area, crystallite sizes, conductivity measurement, packing density, true density and scanning electron microscopy.

2. Experimental techniques

Akaganeite is precipitated from dilute $FeCl_3$ solution at pH 7.0 and 70° C temperature by a homogeneous precipitation method using the urea hydrolysis technique. The method of preparation and the physico-chemical characterization of the samples were described in detail in Part 1 [9].

2.1. Physical measurements

The powdered sample was heated at different temperatures in the range 50 to 1000° C for 5 h in an electric furnace maintained at ± 5° C. The sample was cooled in a desiccator and stored in covered glass tubes. X-ray diffraction patterns of the powdered samples were taken using a Phillips semi-automatic X-ray diffractometer with an auto-divergent slit and a graphite monochromator using Cu$K\alpha$ radiation, operated at 40 kV and 20 mA. The average crystallite sizes of the samples heated to different temperatures were determined by X-ray diffraction line broadening technique using the relation $\beta_{1/2} = 0.94\lambda/D \cos\theta$, where λ is the wavelength of the X-ray used, D is the average diameter of the crystallites and $\beta_{1/2}$ is the width measured at half height of a peak of the sample.

Infrared spectra were recorded using KBr pellets on a Nicolet 170 SX, FT-infrared spectrometer in the range 4000 to 400 cm^{-1}. The scanning electron micrographs were taken using a Siemens Autoscan SEM. Surface area was measured with the help of a high-speed surface area analyser (Micromeritics Instrument Corporation, USA, model no. 2202) using a low-temperature (− 196° C) nitrogen adsorption method.

The pellets (2 cm diameter × 0.2 cm thick) of heat-treated samples were prepared by applying a pressure of 5 ton cm^{-2}. The pellets were coated with a thin layer of silver paint and kept pressed in between the copper disc electrodes; the resistance was determined at room temperature in a conductivity cell using a meg-ohm bridge.

Packing density was measured by packing a known amount of the sample in a 10 ml measuring cylinder and applying 50 to 60 gentle taps within which minimum packing volume was reached. The packing volume was noted with an accuracy of ± 0.1 ml. Density was determined by the pycnometric method by displacement of pure toluene at 26 to 27° C (density of toluene was 0.8604 g cm^{-3} at 27° C).

2.2. Chemical analysis

Total Fe^{3+} in an aliquot was estimated by reduction with stannous chloride and titration with dichromate using barium sulphonate as indicator [10]. The chloride content was estimated using the same method

0022–2461/88 $03.00 + .12

TABLE I Physico-chemical measurements of thermally treated akaganeite samples

Sample	Temperature (°C)	Fe^{3+} content (%)	Cl^- content (%)	Cl^-/Fe^{3+}	Weight loss (%)	Surface area ($m^2 g^{-1}$)	Packing density ($g ml^{-1}$)	Crystallite size (nm)	Conductivity (10^7 mho cm^{-1})
(a)	50	57.55	6.65	0.115	–	21.01	0.972	58.07	54.71
(b)	120	58.62	6.78	0.115	1.81	38.67	0.981	34.84	35.33
(c)	200	60.51	5.76	0.095	9.77	78.79	0.943	24.02	29.41
(d)	300	69.10	1.19	0.017	16.91	7.99	0.909	38.75	3.11
(e)	400	69.46	1.10	0.016	17.13	7.89	0.924	31.73	12.37
(f)	500	69.64	0.695	0.010	17.63	7.57	0.937	30.28	14.51
(g)	600	69.99	0.048	0.0007	17.85	7.26	0.956	31.72	19.74
(h)	800	70.29	0.012	–	18.21	4.31	0.961	31.72	21.85
(i)	1000	70.95	–	–	18.94	0.64	2.129	31.72	25.69

as adopted by Ellis *et al.* [11]. An accurately weighed quantity (about 100 mg) of sample was taken in a glass ampoule and treated with 2 ml 20% sulphuric acid. The sealed ampoule was heated at 100° C in a water bath until a clear solution was obtained. The ampoule was cooled and the contents diluted to 50 ml with 1 M monosodium citrate. The chloride content was determined by direct measurement in a specifix ion meter (Model 407 A) using an orion model 90-02 double-junction reference electrode.

3. Results and discussion

3.1. Chemical analysis

It has been observed from chemical analysis (Table I) that there is a sharp drop in the ratio of chloride to iron between 200 and 300° C, followed by slow decrease up to 600° C. Because chloride ions stabilize the tetragonal structure of β-FeOOH [11], the escape of the ion at 300° C changes the structure from tetragonal to rhombohedral. According to Ellis *et al.* [11], the rapid decrease in Cl^- content is presumably associated with the external surface of the crystal while the slow decrease comes from the hollandite tunnels and perhaps also the longer structural tunnels. The Fe^{3+} and weight loss in Table I show that the samples lose oxygen during heating and the loss begins after 500° C.

3.2. X-ray diffraction patterns

The X-ray diffraction patterns of akaganeite heated to different temperatures (50 to 1000° C) are shown in Fig. 1. The X-ray *d*-values of all the samples are compared with the standard *d*-values of β-FeOOH, α-Fe_2O_3 γ-Fe_2O_3 and δ-Fe_2O_3. The X-ray diffraction pattern of the sample heated at 120° C (b), is little different from the sample heated at 50° C (a). Although some peaks have disappeared and the intensity of the peaks is reduced, there is no change in phase. Broad and low-intensity X-ray diffraction peaks of the sample heated at 200° C (c) are characteristics of β-FeOOH. According to Acharya and Pradhan [12] the highest X-ray line broadening at 200° C is due to particle size broadening and root-mean square strain. Thus akaganeite undergoes a crystal structural change at 200° C without a break in structure. As the broadening effect decreases on further heating some authors [13, 14] believe that this nonuniform broadening is correlated to some crystal imperfections, strains or faults occurring at low decomposition temperatures. Naono and Fujwara [15] correlated the nonuniform broadening to the presence of slit-shaped micropores in acicular haematite crystals. However, Duvigneaud and Derie [16] have recently shown that the nonuniform broadening is due to shape anisotropy of the particles, rather than to strain and fault broadening, because (i) the phenomenon was negligible in spherical-shaped particles; (ii) the non-uniform broadening remains in acicular particles after further heating at 600° C; and (iii) a good estimate of the ratio of the particle width and thickness was found. They concluded that as in this case, the haematite acicular particles were lath-shaped. In agreement with Duvigneaud and Derie [16], the non-uniform broadening remains even at 600° C prior to the sintering process which affects the particle lath morphology.

Temperature has a prominent effect on the crystallite size of β-FeOOH. As the heat-treatment temperature increases, the size of the crystallites perpendicular to (2 1 1) decreases until a temperature of 200° C reached, thereafter it increases again at 300° C and remains constant after 400° C (Table I). The decrease of crystallite size at 200° C is due to the formation of a mesocrystalline structure, and the increase of crystallite size at 300° C is probably due to complete transformation to α-Fe_2O_3.

The unit cell parameters of samples (a) to (i) belonging to two crystal systems are shown in Table II. The least-square unit cell refinement was carried out using a suitable FORTAN IV program for each crystal system by feeding in the observed $h\,k\,l$ and θ values and allowing the computer to calculate a_0, c_0 and unit cell volume values. Unit cell volume remains almost unchanged while c_0 gradually decreases and a_0 gradually increases with increasing heat-treatment temperature up to 200° C. Similar observation was also found by Rendon *et al.* [17] for α-FeOOH. Thus it is concluded that haematite is formed in a closed orientation relationship in the direction of the *c*-axis. The transformation to α-Fe_2O_3 is completed at 300° C and the diffraction patterns (d) to (i) confirm the presence of α-Fe_2O_3. The unit cell parameters of the hexagonal–rhombohedral system remain almost the same up to 800° C and then decrease at 1000° C due to appreciable loss of atomic oxygen.

The infrared spectra of (a) and (c) show broad absorption maximum around 3400 cm^{-1} due, in part, to adsorbed water which also gives rise to the band at 1635 cm^{-1} (see Fig. 2). The areas of the 3400 and 1635 cm^{-1} peaks were less in the case of (c) (heated at 200° C) compared to the original sample (a) (dried at

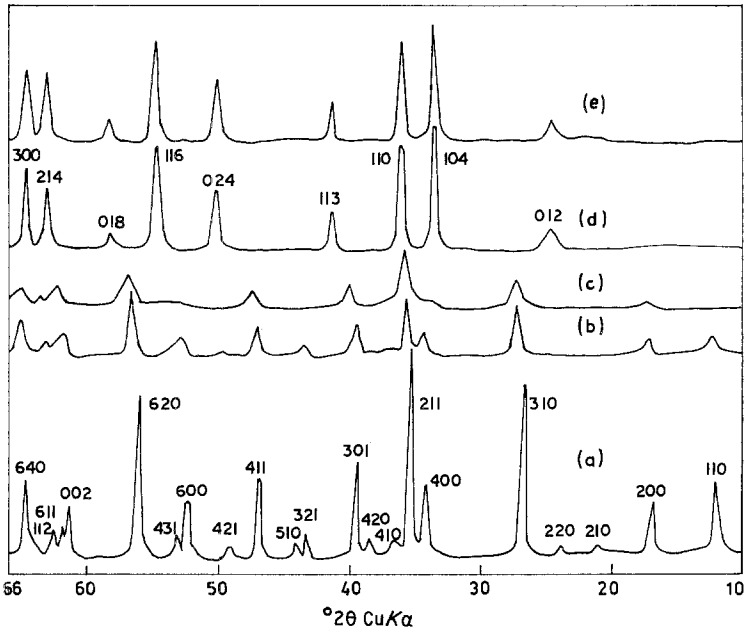

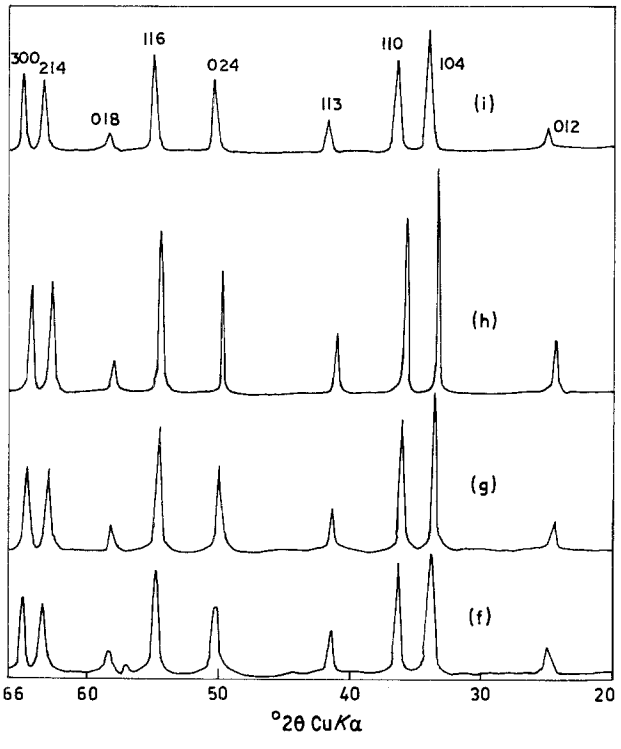

Figure 1 XRD powder patterns of samples (a) to (i) obtained by heating β-FeOOH in air for 3 h. (a) 50° C, (b) 120° C, (c) 200° C, (d) 300° C, (3) 400° C, (f) 500° C, (g) 600° C, (h) 800° C, (i) 1000° C.

50° C). According to Glemser and Reick [18] the O–H stretching vibrations at 3200 to 3500 cm^{-1} are very broad and are obscured by large amounts of adsorbed water which cannot be removed without changes in structure. Samples (a) and (c) also show very weak absorptions around 2350 and 1400 cm^{-1}. The weak absorptions at about 1350 and 1490 cm^{-1} are peculiar to β-FeOOH and are potentially useful for identification [1]. The OH or O–H . . . O bending vibrations were found at 890, 796, 688 and 634 cm^{-1} in the case of sample (a), and at 890, 805, 695 and 634 cm^{-1} in the case of sample (c). Characteristic absorption bands due to lattice vibrations occur at 440 and 427 cm^{-1} in the case of (a) and (c), respectively. Similar observations were also found by Muller [19]. The four peaks in the OH bending vibration region possibly arise from the interactions between the channel water molecules and the lattice of the hollandite structure of β-FeOOH [19]. Samples (g) and (i), heat-treated at 600 and 1000° C, respectively, do not possess O–H . . . O bending vibrations but have only broad lattice peaks at about 570 and 480 cm^{-1} which are characteristic of α-Fe_2O_3. The lattice peak has been shifted to 544 cm^{-1} in the case of (i) due to sintering and mesopore formation. Ionic powders usually show broad absorption bands, resumably due to a large anharmonicity contribution [20] or to particle aggregation [21].

Scanning electron micrographs (Fig. 3a) show that the particles of the original sample (a) are acicular and larger than (c), (g) and (i). According to Gallagher *et al.* [22] β-FeOOH particles are uniform and do not contain typical rods or tactoids. The external

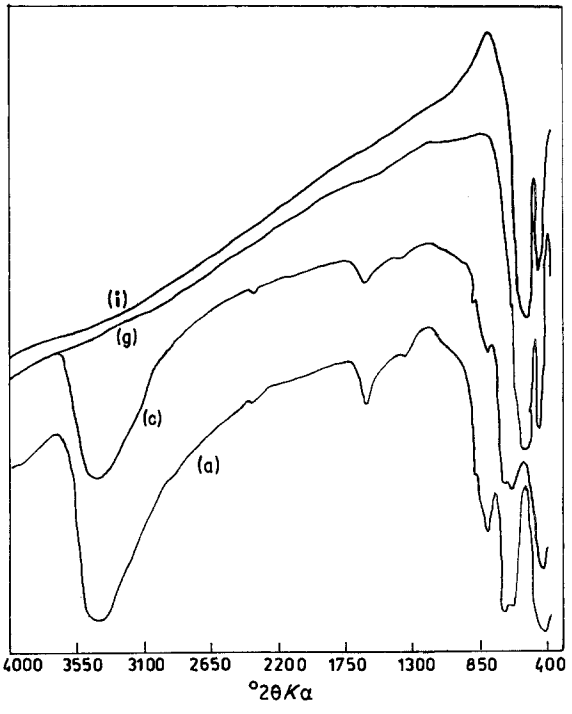

Figure 2 Infrared spectra of samples (a), (c), (g) and (i) obtained by heating β-FeOOH in air for 3 h.

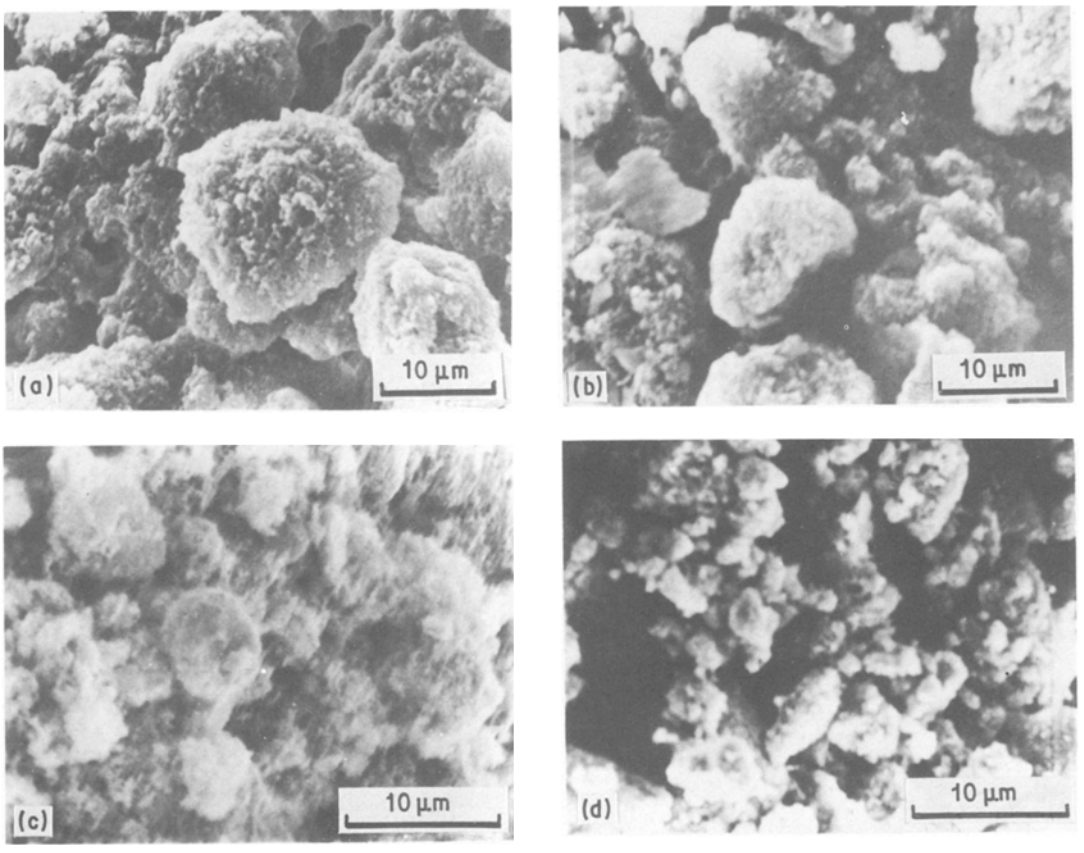

Figure 3 Scanning electron micrographs of samples (i) (a) 50° C, (ii) (c) 200° C, (iii) (g) 600° C and (iv) (i) 1000° C.

appearance of the meso-crystalline sample (Fig. 3b) resembles that of the original akaganeite, i.e. the decomposition reaction occurs within a microcrystal without significant changes in shape. Fig. 3c shows the growth of well-formed hexagonal platelets which are the typical crystal habit of α-Fe_2O_3. Interparticle sintering occurs at 1000° C and leads to heterogeneity in particle size and shape (Fig. 3d).

The conductivity decreases from (a) to (d) and thereafter increases from (e) to (i) (Table I). The higher conductivity of samples from (a) to (d) is due to the presence of moisture and hydroxyl groups. Gradual decomposition of hydroxide and the loss of moisture reduce conductivity as observed between (a) and (d). The sharp decrease in conductivity between (c) and (d) is due to the transformation of mesocrystalline akaganeite to haematite. Removal of small quantities of surface oxygen atoms, as reflected from percentage weight loss, may be the reason for the observed rise in conductivity from (e) to (i).

The surface area increases between 50 to 200° C heat-treatment and thereafter decreases up to 1000° C. Similar to α-FeOOH [17], the surface area of microcrystals increases remarkable at 200° C in the dehydration process of β-FeOOH due to the micropore formation and crystallinity change (mesocrystalline) during akaganeite decomposition. The decrease in surface area from 300 to 1000° C is due to (i) the crystallization of haematite, (ii) the destruction of micropores and their transformation into closed spherical mesopores due to internal sintering which brings about more crystal homogeneity. The packing density decreases with increase in temperature of heat-treatment up to 300° C and thereafter increases up to 1000° C, just like conductivity. The pycnometric density of sample (c) heated at 200° C is lowest due to mesocrystalline phase formation and then increases at 300 to 400° C due to haematite formation and crystallization. The pycnometric density increases between 500 and 1000° C due to the loss of atomic oxygen.

TABLE II Unit-cell parameters of thermally treated akaganeite samples

Sample	Temperature (° C)	Crystal system	a_0 (nm)	c_0 (nm)	Cell volume (nm^3)	Pycnometric density ($g\,cm^{-3}$)
(a)	50	Tetragonal	1.0265	0.3037	0.320009	3.68
(b)	120	Tetragonal	1.0325	0.3034	0.323755	3.90
(c)	200	Tetragonal	1.0330	0.3018	0.322047	3.50
(d)	300	hexagonal–rhombohedral	0.4990	1.3717	0.295786	4.92
(e)	400	hexagonal–rhombohedral	0.5012	1.3746	0.29903	4.97
(f)	500	hexagonal–rhombohedral	0.5007	1.3723	0.297935	4.98
(g)	600	hexagonal–rhombohedral	0.5012	1.3755	0.299226	5.35
(h)	800	hexagonal–rhombohedral	0.5012	1.3749	0.299096	5.42
(i)	1000	hexagonal–rhombohedral	0.5000	1.3688	0.295912	5.57

Acknowledgements

The author thanks Dr S. B. Rao for constant encouragement during the course of this investigation, Mr A. Suryanarayana for helpful discussions, and Professor P. K. Jena, Director, Regional Research Laboratory, Bhubaneswar for his keen interest and kind permission to publish this paper.

References

1. K. KAUFFMAN and F. HAZEL, *J. Inorg. Nucl. Chem.* **37** (1975) 1139.
2. E. MURAD, *Clay Minerals* **14** (1979) 273.
3. N. NAGAI, N. HOSOITO, M. KIYAMA, T. SHINJO and T. TAKADA, Ferrites: Proceedings of the International Conference, Japan, edited by H. Watanabe *et al.* (1982) p. 247.
4. I. DEZSI, L. KESZTHELYI, D. KULGAWCZUK, B. MOLNAR and N. A. EISSA, *Phys. Status Solidi* **22** (1967) 617.
5. T. ISHIKAWA and K. INOUYE, *Bull. Chem. Soc. Jpn* **48** (1975) 1580.
6. A. L. MACKAY, *Miner. Mag.* **32** (1960) 545.
7. H. BRAUN and K. J. GALLAGHER, *Nature* **240** (1972) 1923.
8. D. G. CHAMBAERA and E. DE GRAVE, *Phys. Chem. Miner.* **12** (3) (1985) 176.
9. K. M. PARIDA, *J. Mater. Sci.* **23** (1988) in press.
10. A. I. VOGEL, "Quantitative Inorganic Chemical Analysis" (ELBS and Longman, 1969) p. 310.
11. J. ELLIS, R. GIOVANOLI and W. STUMM, *Chimia* **3** (1976) 30.
12. B. S. ACHARYA and L. D. PRADHAN, *J. Appl. Crystallogr.* **19** (1986).
13. H. P. ROOKSBY, in "X-ray Identification and structures of Clay Minerals", (Mineralogical Society, London, 1961) p. 376.
14. G. W. VAN OOSTERHOUT, *Acta Crystallogr.* **13** (1960) 932.
15. N. NAONO and R. FUJIWARA, *J. Colloid Interface Sci.* **73** (1980) 406.
16. P. H. DUVIGNEAUD and R. DERIE, *J. Colloid State Chem.* **34** (1980) 323.
17. J. L. RENDON, J. CORNEJO, P. DE ARAMBARRI and C. J. SERNA, *J. Colloid Int. Sci.* **92-2** (1983) 508.
18. O. GLEMSER and R. G. RIECK, *Z. Anorg. Allg. Chem.* **297** (1958) 175.
19. A. MULLER, *Arzneimittal – Forsch* **8** (1967) 921.
20. L. GANZEL and T. P. MARTIN, *Phys. Status Solidi (b)* **51** (1972) 91.
21. P. CLIPPE, E. EVRARD and A. A. LUCAS, *Phys. Rev. E* **14** (1976) 1715.
22. K. J. GALLAGHER and D. N. PHILLIPS, *Chimia* **23** (1969) 465.

Received 14 January
and accepted 16 June 1987